Targeted VEGF therapy induces long-term renal recovery in chronic kidney disease via macrophage polarization

Jason E. Engel[1]

Erika Williams[1]

Maxx L. Williams, MS[1]

Gene L. Bidwell III, PhD[2,3,4]

Alejandro R. Chade, MD, FAHA[1,5,6]

The Department of Physiology and Biophysics[1], the Department of Neurology[2], the Department of Cell and Molecular Biology[3], the Department of Pharmacology and Toxicology[4], the Department of Medicine[5], and the Department of Radiology[6], University of Mississippi Medical Center, Jackson, MS.

Short title: VEGF therapy in CKD

Word count: 2,482 (text, figure legends, references)

Total number of supplementary figures/videos: 3

Correspondence:
Alejandro R. Chade, MD, FAHA
Professor
Department of Physiology and Biophysics, Medicine, and Radiology
University of Mississippi Medical Center
2500 North State Street, Jackson, MS, 39216-4505.
Phone: (601)-984 2898; Fax: (601)-984 1817
achade@umc.edu

Supplemental Material:

1) **Extended methods**
2) **Supplementary Video and Figure**

1a. Experimental Design

All studies were approved by the Institutional Animal Care and Use Committee at the University of Mississippi Medical Center. Twenty-one juvenile pigs (*sus scrofa domesticus*) were studied for a total of 14 weeks. We induced CKD in 14 pigs through bilateral renal artery stenosis and a high cholesterol diet (15% lard, 2% cholesterol; Envigo, NJ) that was initiated immediately after induction of the stenosis and maintained for 14 weeks, as recently described[1]. Briefly, pigs were fasted overnight, and anesthesia was induced with intramuscular ketamine and maintained with a mixture of ketamine and xylazine in saline (3 mL/min IV). Under sterile conditions, a 7-mm angioplasty balloon containing a copper coated wire coil was passed from the femoral artery into the proximal-middle renal artery over a 0.014" guide wire and inflated to 14 atm to expand the coil. The balloon was then deflated and removed, leaving the coil in place. This process was repeated in the main artery of the other kidney. The coil induces a progressive narrowing of the renal artery with increased blood pressure detectable within 10 days post-op[2-6]. Blood pressure was measured continuously by telemetry (Data Sciences International, St. Paul, MN), as described[3, 5]. An additional 7 pigs underwent sham surgery, were fed a normal diet, and served as normal controls.

Six weeks after induction of CKD, pigs were anesthetized with intramuscular telazol (5 mg/kg) and xylazine (2 mg/kg), intubated, and mechanically ventilated. Anesthesia was maintained with a ketamine (0.2 mg/kg/min) and xylazine (0.03 mg/kg/min) mixture in normal saline administered via an ear cannula. Under fluoroscopic guidance, a 5F pigtail catheter was passed through the external jugular vein into the right atrium for contrast injection. Pigs then underwent contrast-enhanced multidetector computed tomography (MDCT) to quantify renal blood flow (RBF) and glomerular filtration rate (GFR, described below). Following quantification of renal function at 6 weeks, a 7F balloon catheter was advanced from the carotid into the main renal artery (left or right, random), inflated slightly to occlude flow, and ELP-VEGF (100 μg/kg) or vehicle was injected through the balloon lumen into the kidney over two minutes. The dose was selected based on our previous study showing therapeutic renoprotective effects in the stenotic kidney of the swine model of renal artery stenosis[5]. Renal hemodynamics and function was again quantified at 10 and 14 weeks (4 and 8 weeks post-treatment respectively). Blood and urine were collected to assess albuminuria, serum creatinine, and urinary markers of renal injury neutrophil gelatinase-associated lipocalin (NGAL) and kidney injury molecule-1 (KIM-1).

After 14 weeks of observation, pigs were euthanized by an intravenous overdose of phenobarbital (100 mg/kg). Kidneys were harvested. One pole was snap frozen in liquid nitrogen for *ex vivo* assays, mid-hilar sections were preserved in formalin for histology, and one pole was prepared for Micro-CT scanning to quantify renal MV density.

1b. *In vivo* studies: Renal Function

Renal hemodynamics and filtration were quantified *in vivo* using MDCT (SOMATOM Sensation 64, Siemens Medical Solutions, Germany). Manually traced regions of interest from each kidney and each region were selected and time-density curves were generated using ANALYZE™ (Biomedical Imaging Resource, Mayo Clinic, Rochester, MN). Time-density curves were plotted to calculate RBF, GFR, total and regional perfusion, as previously shown

and validated [1,2,5,7-10]. Cortical and medullary volume of each kidney was quantified, and renal vascular resistance calculated, as previously shown[1,5,7,9,10]. Seven normal, seven CKD and seven CKD ELP-VEGF animals were used to quantify renal hemodynamics (Note: one pig from the CKD-ELP-VEGF group died unexpectedly on week 12, resulting in n=6 at the 14-week timepoint for that group only)

1c. *Ex Vivo Studies*

1c-1. Renal microvascular density and architecture

Following euthanasia, kidneys were perfused with heparinized saline followed by a polymer contrast agent (Microfil MV122, Flow Tech, Carver, MA). After 72 hour fixation in formalin, samples were scanned using a Micro-CT (SkyScan 1076, Bruker Biospin Corp., MA) at 0.3° increments at a resolution of 9 μm. ANALYZE™ (Biomedical Imaging Resource, Mayo Clinic, Rochester, MN) was used to generate 3D reconstructions and subsequently quantify MV density of microvessels between 0-500 μm in the cortex and medulla, as described[1,4,5,8]. Seven normal, seven CKD and six CKD+ELP-VEGF samples were used.

1c-2. Protein expression

Standard western blotting was performed using renal tissue homogenates (mainly cortex0, as described[1,5,6] to quantify expression of VEGF (1/250, sc-507, Santa Cruz, CA), its receptor Flk-1 (1/1000, sc-505, Santa Cruz), total and phosphorylated (p) renal expression of the inflammatory mediator nuclear factor kappa B (NF-κB, 1/1000, ab86299, Abcam, MA, **Figure S1**), and its inhibitor IkB (1/1000, ab97783, Abcam; **Figure S1**), as well as pro-fibrotic factors transforming growth factor-β (TGF-β, 1/800, ab92486, Abcam), connective tissue growth factor (CTGF, 1/500, OAAB09712, Aviva Systems Biology, CA), and tissue inhibitor of metalloproteinase-1 (TIMP-1, 1/1000 sc-5538, Santa Cruz). Protein expression was quantified relative to beta-actin (1/1000, sc-47778, Santa Cruz), except for p- NF-κB that was expressed as p-NFkB/IkB ratio. Five normal, six CKD, and six CKD+ELP-VEGF samples were used in each western blot gel. Figures show 2 representative bands per group.

1c-3. Immunohistochemistry

Paraffin-embedded mid-hilar 5 μm kidney sections from each animal were used to perform immunohistochemistry, as detailed[1], for CD68 (green, 1/50, BA4D5, Bio-Rad, CA), indoleamine-2,3-dioxygenase (IDO, red, 1/50, LS-B1746, LSBio, WA), and mannose receptor-c type 1 (MRC1, blue, 1/50, LS-B9805, LSBio) to identify M1 and M2 macrophage infiltration. IDO and MRC1 were chosen as markers of M1 and M2 macrophages respectively as their expression is highly conserved between pigs and humans[11-13]. We note that M1 and M2 markers reflect a general inflammatory or trophic phenotype but may not be macrophage specific. Fortunately, MRC1 was macrophage specific in our study. However, IDO demonstrated clustered tubular staining, most pronounced in untreated CKD animals. This is consistent with studies showing IDO is upregulated in damaged renal tubules, facilitating epithelial-to-mesenchymal transition[14,15]. This nonspecific staining made addition of a macrophage specific marker (CD68) necessary. Kidney sections were concurrently stained with mouse anti-CD68, rabbit anti-MRC1, and goat anti-IDO followed by species appropriate Alexa Fluor-488, 547, and Cy5 secondary antibodies. Sections were then analyzed under a Leica TCS SP8 confocal microscope (Leica Microsystems Inc., IL). Cells which were positive for both CD68 and IDO or MRC1 were considered M1 or M2 macrophages respectively. Cells were counted in 15 randomly selected high-power fields per slide and expressed as number of dual positive cells per field. Seven normal, seven CKD and six CKD+ELP-VEGF samples were used.

These experiments on M1 and M2 macrophages were extended by a set of renal sections

(7 normal, 7 CKD and 6 CKD+ELP-VEGF) co-stained with another M1 marker (CD86, 1/50, LS-B11911, LSBio), a M2 marker (MRC1), and an antibody against NF-κB (1/100, LS-C290611, LSBio). Regions of interest were manually traced over individual macrophages to quantify mean fluorescence intensity of NF-κB using confocal microscopy **(Figure S1)**.

Furthermore, another set of renal sections were used to co-stain M2 (MRC1) macrophages and VEGF (1/100, VG76e, Abcam) and the nuclear stain DAPI. Macrophages co-expressing MRC1-VEGF were identified by confocal microscopy and display in a full 3D z-stack.

1c-4. M2 VEGF Colocalization Z-Stack (Supplementary video file, SV1)

Paraffin embedded renal sections were stained for mannose receptor c type-1 (MRC1, green) to label M2 macrophages, vascular endothelial growth factor A (VEGFA, red) and the nuclear marker DAPI (blue). A 50-image z-stack was collected of a glomerulus in an ELP-VEGF treated pig. The video attached to this supplementary file shows the full z-stack in 3D and zooms in on a glomerular M2 macrophage expressing surface MRC1 and high levels of intracellular VEGFA, another M2 with some VEGF expression, and lastly, areas of VEGFA staining without colocalized MRC1, likely derived from endothelial cells or podocytes. These VEGF expressing macrophages were rarely or not at all observed in untreated CKD animals.

1c-5. Renal morphometric analysis

Mid-hilar paraffin-embedded 5 μm kidney sections from each pig were stained with trichrome[1, 16] and morphometric analysis was performed using Image J (National Institutes of Health, USA) to quantify glomerulosclerosis, tubulointerstitial fibrosis, and media-to-lumen ratio, as described[17, 18]. Seven normal, seven CKD and six CKD+ELP-VEGF samples were used.

1c-6. Statistical analysis

Power analysis of prior renal hemodynamics data revealed that a minimal n=6 per group was sufficient to detect a difference of 11% among groups at 80% power with an alpha=0.05 Results are expressed as mean ± SEM. Treatment groups were compared using one-way ANOVA with post-hoc Tukey's or Fisher (as indicated in Figure legends) for multiple comparisons. Statistical significance was accepted for $p \leq 0.05$.

1d. *In vitro* studies: VEGF and macrophage polarization

THP-1 human monocytes were cultured in complete RPMI 1640 containing glutamine, HEPES, and 10% fetal bovine serum. Upon reaching confluence, cells were seeded in three 6 well plates at a density of 1.5×10^6 cells per well. All plates were incubated in complete RPMI containing 100 nM phorbol 12-myristate-13-acetate for 48 hours to induce differentiation to naive macrophages[19]. One plate was then incubated with media containing 20 ng/mL IFNγ and 100 ng/mL LPS for 48 hours to induce M1 differentiation[20] while the remaining two plates received normal media. Lastly one plate of M1 macrophages and one plate of M0 macrophages were incubated in media containing 4 μg/mL of recombinant human VEGF[20] for 48 hours while the remaining plate received normal media. During this final 48-hour incubation, cells were kept in a hypoxic incubator at 1% O2. Following this incubation, cDNA was produced from cell lysate according to manufacturer instructions (PureLink RNA Mini Kit, Thermo Fisher Scientific) and PCR was performed to quantify expression of VEGF (Thermo Fisher Scientific, assay ID Hs00900055_m1) and MRC1 (Thermo Fisher Scientific, assay ID Hs00267207_m1) mRNA relative to beta actin using the $2^{-\Delta\Delta Ct}$ method. Results were expressed relative to untreated M0 macrophages and now shown in Supplementary Figure 2.

References

1. Chade AR, Williams ML, Engel J, et al. A translational model of chronic kidney disease in swine. *American journal of physiology Renal physiology*. 2018;315:F364-f373.
2. Lerman LO, Schwartz RS, Grande JP, et al. Noninvasive evaluation of a novel swine model of renal artery stenosis. *Journal of the American Society of Nephrology : JASN*. 1999;10:1455-1465.
3. Chade AR, Rodriguez-Porcel M, Grande JP, et al. Distinct renal injury in early atherosclerosis and renovascular disease. *Circulation*. 2002;106:1165-71.
4. Chade AR, Kelsen S. Reversal of renal dysfunction by targeted administration of VEGF into the stenotic kidney: a novel potential therapeutic approach. *American journal of physiology Renal physiology*. 2012;302:F1342-50.
5. Chade AR, Tullos NA, Harvey TW, et al. Renal Therapeutic Angiogenesis Using a Bioengineered Polymer-Stabilized Vascular Endothelial Growth Factor Construct. *Journal of the American Society of Nephrology : JASN*. 2016;27:1741-52.
6. Chade AR, Williams ML, Guise E, et al. Systemic biopolymer-delivered vascular endothelial growth factor promotes therapeutic angiogenesis in experimental renovascular disease. *Kidney Int*. 2018;93:842-854.
7. Chade AR, Zhu X, Lavi R, et al. Endothelial progenitor cells restore renal function in chronic experimental renovascular disease. *Circulation*. 2009;119:547-57.
8. Chade AR, Zhu X, Mushin OP, et al. Simvastatin promotes angiogenesis and prevents microvascular remodeling in chronic renal ischemia. *FASEB journal : official publication of the Federation of American Societies for Experimental Biology*. 2006;20:1706-8.
9. Daghini E, Primak AN, Chade AR, et al. Assessment of renal hemodynamics and function in pigs with 64-section multidetector CT: comparison with electron-beam CT. *Radiology*. 2007;243:405-12.
10. Krier JD, Ritman EL, Bajzer Z, et al. Noninvasive measurement of concurrent single-kidney perfusion, glomerular filtration, and tubular function. *American journal of physiology Renal physiology*. 2001;281:F630-8.
11. Meng XM, Tang PMK, Li J, et al. Macrophage Phenotype in Kidney Injury and Repair. *Kidney Diseases*. 2015;1:138-146.
12. Kapetanovic R, Fairbairn L, Beraldi D, et al. Pig Bone Marrow-Derived Macrophages Resemble Human Macrophages in Their Response to Bacterial Lipopolysaccharide. *The Journal of Immunology*. 2012;188:3382-3394.
13. Schroder K, Irvine KM, Taylor MS, et al. Conservation and divergence in Toll-like receptor 4-regulated gene expression in primary human versus mouse macrophages. *Proceedings of the National Academy of Sciences of the United States of America*. 2012;109:E944-53.
14. Mohib K, Wang S, Guan Q, et al. Indoleamine 2,3-dioxygenase expression promotes renal ischemia-reperfusion injury. *American journal of physiology Renal physiology*. 2008;295:F226-34.
15. Matheus LHG, Simao GM, Amaral TA, et al. Indoleamine 2, 3-dioxygenase (IDO) increases during renal fibrogenesis and its inhibition potentiates TGF-beta 1-induced epithelial to mesenchymal transition. *BMC nephrology*. 2017;18:287.
16. Chade AR, Tullos N, Stewart NJ, et al. Endothelin-a receptor antagonism after renal angioplasty enhances renal recovery in renovascular disease. *Journal of the American Society of Nephrology : JASN*. 2015;26:1071-80.
17. Tullos NA, Stewart NJ, Davidovich R, et al. Chronic blockade of endothelin A and B

receptors using macitentan in experimental renovascular disease. *Nephrol Dial Transplant*. 2015;30:584-93.
18. Chade AR, Kelsen S. Renal microvascular disease determines the responses to revascularization in experimental renovascular disease. *Circulation Cardiovascular interventions*. 2010;3:376-83.
19. Daigneault M, Preston JA, Marriott HM, et al. The identification of markers of macrophage differentiation in PMA-stimulated THP-1 cells and monocyte-derived macrophages. *PloS one*. 2010;5:e8668.
20. Wheeler KC, Jena MK, Pradhan BS, et al. VEGF may contribute to macrophage recruitment and M2 polarization in the decidua. *PloS one*. 2018;13:e0191040.

2) Supplementary Figures and Video

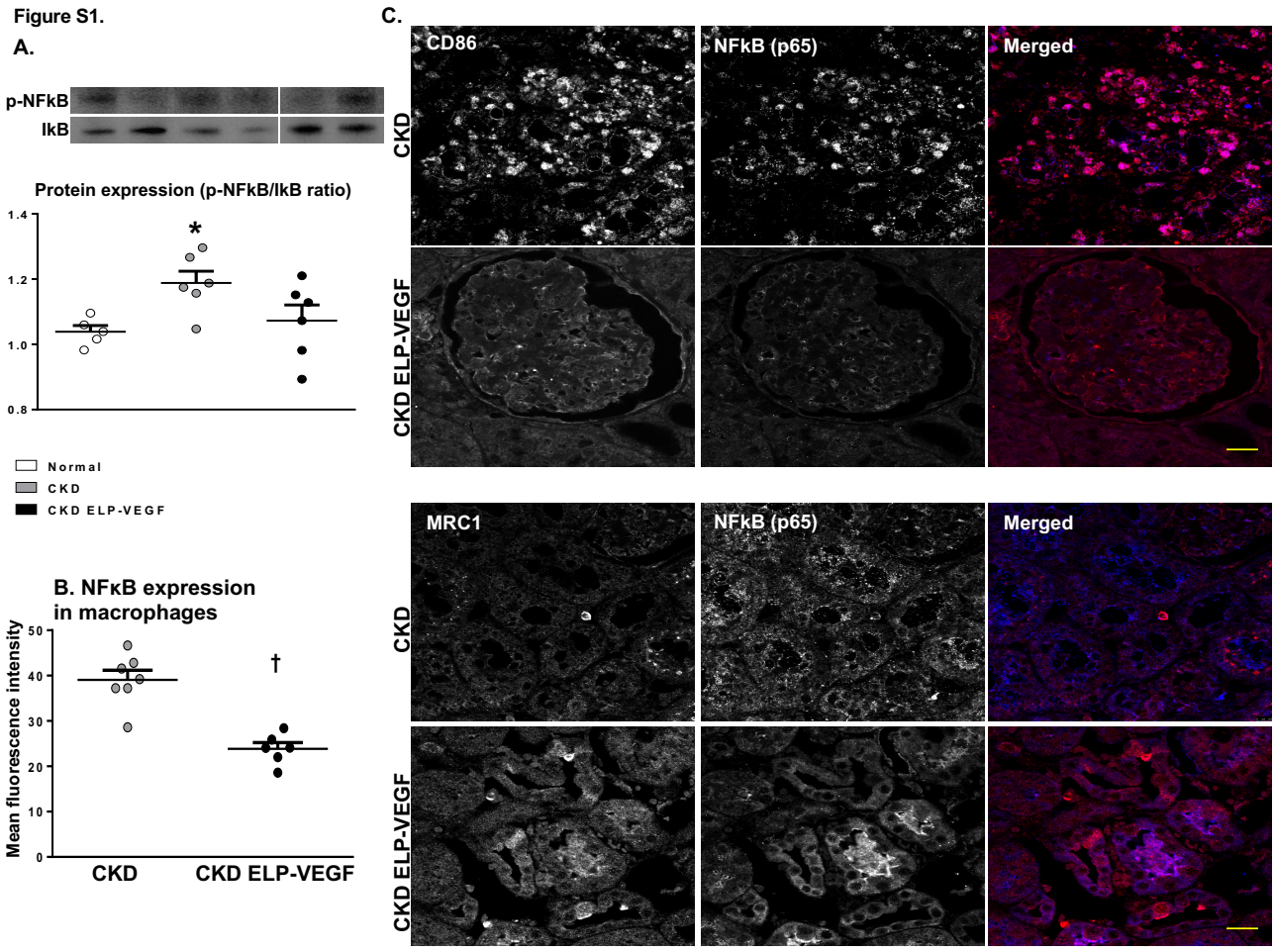

Figure S1. Representative bands (2 per group, n=5-6 total per group) showing renal protein expression and quantification of phosphorylated NF-κB and its inhibitor IκB (p- NF-κB /IκB ratio, A), quantification of NF-κB in renal macrophages (B) and representative immunostaining of M1 (CD86, red) and M2 (MRC1, red) macrophages colocalized with the NF-κB p65 subunit (blue) (C) from normal, CKD, and CKD ELP-VEGF pigs after 14 weeks of observation. NF-κB expression was elevated in CKD and densely colocalized with CD86+ M1 macrophages. Treatment with ELP-VEGF reduced NF-κB expression in the whole kidney and within macrophages. In addition, suppression of NF-κB was noted in zones surrounding M2 macrophages, suggesting attenuation of tissue inflammation and a functional anti-inflammatory shift in macrophage phenotype. Scale bar represents 20 μm. *p<0.05 vs. normal; † p<0.05 vs. CKD (single way ANOVA, Tukey).

Figure S2.

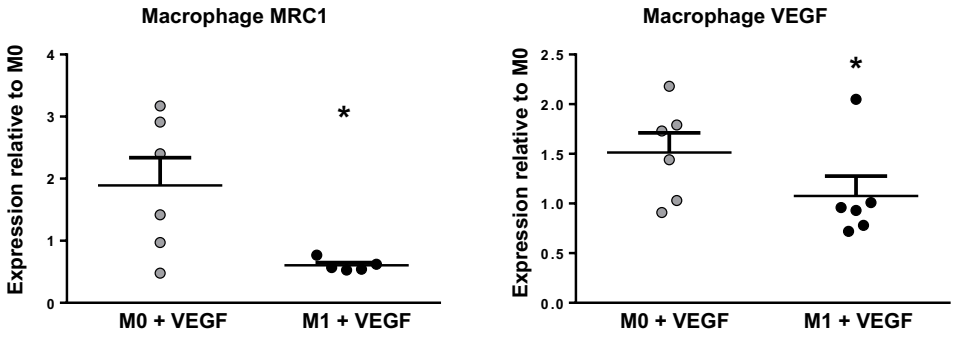

Figure S2. MRC1 and VEGF mRNA expression in M1 vs naïve M0 macrophages treated with VEGF in hypoxic conditions to mimic the ischemic kidney. MRC1 expression increased dramatically in M0 macrophages treated with VEGF while M1s demonstrated nearly no change, suggesting that in a hypoxic setting VEGF may directly induce M2 polarization and that M1s resist this phenotype shift. This shift to an M2 phenotype from M0 cells was associated with significantly increased expression of VEGF mRNA, supporting the conclusion this acute VEGF treatment produces an angiogenic M2 phenotype. *$p<0.05$ vs M0+VEGF (single way ANOVA, Tukey).

Supplementary video (SV1): A) Representative full 3D z-stack of a region from renal cross sections showing co-immunoreactivity for M2 macrophages (MRC1, green), VEGFA (red), and DAPI (blue) from a CKD ELP-VEGF pig after 14 weeks of observation. The video shows glomerular cells displaying co-immunoreactivity of MRC1 and VEGF after with ELP-VEGF therapy, which resulted in a significantly increased VEGF expression inside of M2 macrophages. Accumulation of VEGF-expressing M2 macrophages after ELP-VEGF therapy was also observed in peritubular spaces.